ISSN 1063-7834, Physics of the Solid State, 2012, Vol. 54, No. 2, pp. 360–367. © Pleiades Publishing, Ltd., 2012.
Original Russian Text © B.A. Belyaev, N.A. Drokin, 2012, published in Fizika Tverdogo Tela, 2012, Vol. 54, No. 2, pp. 340–346.

LOW-DIMENSIONAL SYSTEMS

Impedance Spectra of Thin Permalloy Films with a Nanoisland Structure

B. A. Belyaev[a,b,*] and N. A. Drokin[a]

[a] *Kirensky Institute of Physics, Siberian Branch of the Russian Academy of Sciences, Akademgorodok 50–38, Krasnoyarsk, 660036 Russia*

[b] *Reshetnev Siberian State Aerospace University, pr. im. Gazety "Krasnoyarskii Rabochii" 31, Krasnoyarsk, 660014 Russia*

* *e-mail: belyaev@iph.krasn.ru*

Received June 15, 2011

Abstract—The behavior of the impedance spectra of island permalloy films prepared through vacuum evaporation onto optically polished glass-ceramic substrates has been investigated in the frequency range from 0.0001 to 100 MHz. A resistor–capacitor model of the films has been developed and the model parameters, for which there is a good agreement with experimental data on the frequency dependences of the real and imaginary components of the impedance, have been determined. The specific features in the behavior of the electrical and physical characteristics with variations in the thickness of the sample and the gap between the measuring electrodes have been investigated. It has been found that the relative permittivity of the films under investigation reaches values $\varepsilon \sim 10^7$–10^8. The structural relaxation times have been calculated.

DOI: 10.1134/S1063783412020084

1. INTRODUCTION

As is known, nanocrystalline composite materials exhibit unusual electrical and magnetic properties that can be used in the design of new elements for microelectronics. Of great interest, in particular, are ultradispersed mixtures of different substances, nanopowders, nanowires, nanofibers, nanotubes, and nanostructures based on thin metal island films. The nature of some effects observed in thin metal island films has still not clearly understood. In this respect, investigation of these materials is an important problem not only in the applied science but also in the fundamental research. The specific properties of the majority of ultradispersed materials are associated with a substantial increase in the volume fraction of interfaces of structural aggregates with a decrease in their size. This has often led to significant changes in some physical characteristics of the materials. For example, products obtained from these materials, as a rule, possess an increased durability due to a substantial increase in the hardness [1, 2], which, in turn, is caused by the presence of defects with a high density, because boundaries of grains or crystallites have a clearly pronounced nonequilibrium structure. Soft magnetic materials based on multilayer nanocrystalline metal structures have a narrow ferromagnetic resonance (FMR) line and a high magnetic permeability in the microwave frequency range [3] when the sizes of crystallites are considerably less than the correlation length related to the exchange interaction between them [4]. In this case, the observed broadening of the FMR lines due to the random spread in the crystalline anisotropy axes in crystallites is reduced to the value determined by the actual damping in the material used.

However, some specific features of the organization of nanostructures on the surface of the substrate are observed in the synthesis of ultrathin films. In particular, at early stages of the deposition of films (with a thickness as small as several tens of angstroms), there arise spatially separated metal islands that are uniformly distributed over the surface area of the substrate. Undoubtedly, the electrical and physical properties of island films significantly differ from the properties of continuous films, despite the fact that the crystal structure of islands, in the majority of cases, is similar to the structure of the bulk material. Experiments have demonstrated that such structures, according to their properties, are similar to semiconductor materials. In particular, the electrical resistivity of these structures is considerably higher than the electrical resistivity of the bulk material and the electrical conductivity with increasing temperature increases exponentially, because it is frequently determined either by hopping conduction or by tunneling of electrons through potential barriers between the islands [5]. With an increase in the thickness of the films, the islands begin to partially superimpose on one another and, above the percolation threshold, the sample acquires a metallic conductivity.

Modern technological equipment has provided a means for very precisely controlling the process of deposition of films with a specified thickness; as a consequence, such structures are well reproducible and represent convenient objects for physical investigations, as well as for possible technical applications. Owing to the unique electrical and physical properties of island aggregates, these materials can be used as sensors for physical quantities, microelectronics, and spintronics [6]. The island films synthesized under specific technological conditions have a tendency toward self-organization of island aggregates, which makes it possible to design and fabricate structurally ordered nanomaterials for optics, for example, photonic crystals [7, 8]. It has been found that spatially modulated (in thickness) layered structures based on films of ferromagnetic and nonmagnetic metals (Co/Cu, Ni/Cu, etc.) exhibit effects of giant magnetoresistance [9, 10]. Furthermore, recent investigations of the electrical and physical properties of multilayer island films based on Co, W, and FeNi have revealed that these materials possess an anomalously high effective permittivity, which reaches values $\varepsilon \sim 10^7$–10^8 [11].

It should be noted that real island films and the related multilayer systems are far from ideal, both in chemical composition and structure, even on relatively small surface areas. This circumstance is associated, in many respects, with the specific features of the technologies employed for their preparation, as well as with the precise control of the conditions used for the deposition of films, because their variation can lead to significant changes in the electrical and physical characteristics of the samples [12]. In this connection, attempts to generalize the available experimental results and to reveal regularities in the behavior of structural, magnetic, electrical, and other characteristics of the island structures have so far remained problematic.

This work is devoted to the investigation of the electrical impedance spectra of single-layer island FeNi films with different thicknesses, which were prepared through thermal evaporation of permalloy on a dielectric substrate under specific technological conditions. We have experimentally measured the complete resistance $Z^* = Z' + iZ''$ (impedance) for a layered substrate–film structure in the frequency range from 100 Hz to 100 MHz. Here, Z' and Z'' are the active (real) and reactive (imaginary) components of the impedance vector, which allow one to determine and analyze both the dielectric and conductive characteristics of materials [13]. In this paper, we have proposed a resistor–capacitor model of the films and determined the model parameters for which there is a good agreement with measurements, analyzed the obtained results, and discussed some methodological problems of the experiment.

2. SAMPLE PREPARATION AND EXPERIMENTAL TECHNIQUE

Thin films were prepared by the standard method of thermal evaporation of the metal in vacuum [14]. Permalloy of the Ni_{80}–Fe_{20} (wt %) composition was used as the metal, and the chemical vapor deposition was performed onto polished glass-ceramic substrates (0.5 mm in thickness) heated to a temperature of 200°C; the deposition rate was approximately equal to 0.5 nm/s. The deposition rate and the effective thickness of the samples of island films thus prepared were controlled using a KITP-5 quartz film thickness meter in the process of deposition. This instrument was preliminarily calibrated against the results obtained from measurements of reference samples with the use of X-ray fluorescence analysis [15], which made it possible to determine the thickness of films with an accuracy of ±1 nm.

The surface structure of the prepared films with a thickness in the range from 1 to 5 nm was investigated by scanning on an atomic force microscope. A typical pattern of the surface region 15 × 15 μm in size is shown in Fig. 1a for the film with a thickness of 3 nm. Figure 1b presents the cross sections made parallel to the x axis (for $y = 5.2$ μm) and parallel to the y axis ($x = 5.7$ μm), which show the profiles of heterogeneities in the sample. As can be seen from this figure, the maximum values of "overshoots" in height reach 30 nm, whereas the characteristic dimensions of the heterogeneities along the x and y axes are approximately equal to 2–3 μm.

The geometry of the samples under investigation is shown in Fig. 2. Substrate *1* for permalloy film *2* was prepared from a glass-ceramic material with the permittivity $\varepsilon_1 = 10$ in the form of a rectangular plate with dimensions $l \times w \times h_1 = 20 \times 10 \times 0.5$ mm^3. Electrodes *3* with a width of 1 mm and a thickness $h_3 \sim 50$–100 μm were deposited on the surfaces of the films. The electrodes were fabricated from indium, a gold foil, or a kontaktol based on graphite. The distance between the electrodes (r) was varied in the range from 1–10 mm. The electrodes deposited on the sample were connected with conductor wires (~20 mm in length) to WK 4270 (Wayne Kerr Electronics, United Kingdom) and BM 538 (Tesla, Czech Republic) automatic impedance meters operating in the frequency ranges $f = 0.0001$–1 and 1–100 MHz, respectively. The inductance of the wires $L \leq 1$ μH began to make a barely noticeable contribution to the measured values of the impedance only at frequencies $f > 90$ MHz.

In the process of measurement, at each chosen frequency, we measured the impedance modulus $|Z|$ and the phase shift between the electric current and voltage φ. Then, we calculated and plotted the frequency

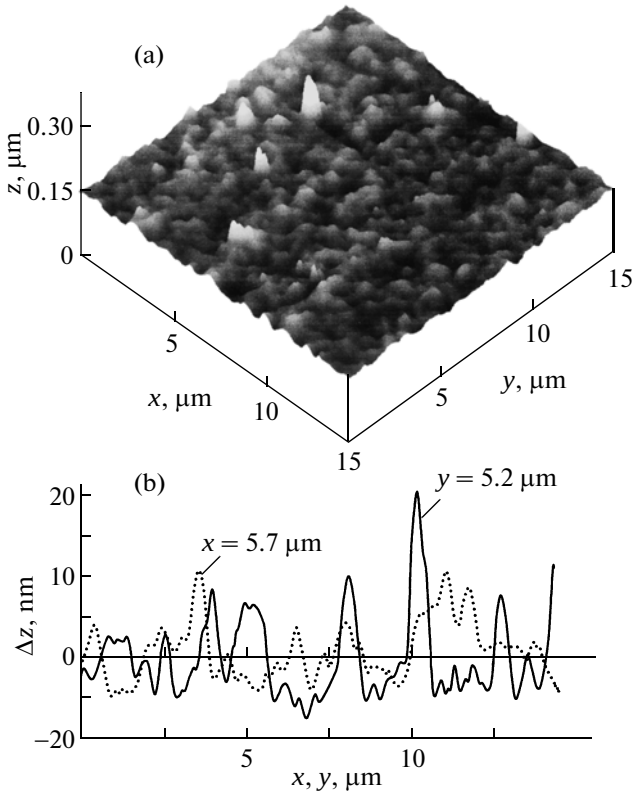

Fig. 1. (a) Fragment of the film surface according to the atomic force microscopy data and (b) profile of roughnesses of the sample with respect to the average level: along the x axis (solid line) and along the y axis (dotted line).

dependences of the real ($Z' = |Z|\cos\varphi$) and imaginary ($Z'' = |Z|\sin\varphi$) components of the impedance. As is known, in the technique employed in impedance spectroscopy for the analysis of the results of measurements, it is necessary to construct a model of the studied object in the form of an electrical circuit consisting of active (resistors) and reactive (capacitors and inductance coils) elements. Furthermore, the electrical circuit itself and the parameters of its elements should be chosen so that the frequency dependences of the real and imaginary components of the impedance of the model thus constructed would be close to those actually measured in the experiment. This approach allows one not only to explain the nature of the observed patterns, when an alternating electric current flows in the sample, but also to calculate the relaxation times of the materials under investigation. The choice of one or another electrical circuit is determined individually for each object, depending on the character of variations in the impedance modulus $|Z|$, the phase shift φ, and the impedance locus constructed in the Z'–Z'' coordinates [16].

In the island films placed in an alternating-current (ac) electric field, on opposite sides of the islands there

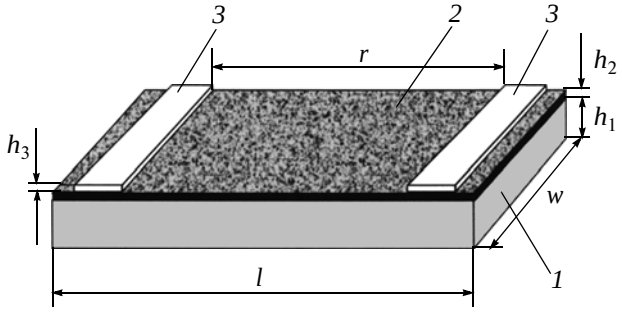

Fig. 2. Schematic drawing of the sample under investigation: (*1*) substrate with the permittivity ε_1, (*2*) Ni_{80}–Fe_{20} permalloy film with the permittivity ε_2, and (*3*) contacts.

arise induced charges; therefore, each pair of oppositely charged regions of the neighboring islands separated by a gap can be considered as a capacitor characterized not only by the loss due to the conduction in the metal but also by the charge "leakage" due to the tunneling conduction of electrons through the potential barrier of the gap. In the framework of this representation, the analysis of the materials under investigation can be performed using a simple equivalent electrical circuit that consists of a capacitor and a resistor connected in parallel with it. However, as will be shown below, this circuit is rather well consistent with the experiment only for very thin samples ($h_2 \le 2$ nm). For "thicker" films, the equivalent electrical circuit should be somewhat complicated, because in these objects there can occur processes of partial coalescence of metal islands and the formation of some heterogeneous planar structures, which can have, first, an inductance and, second, a set of relaxation times. It is important to note that, sometimes, it is also necessary to take into account the influence exerted on the measured impedance by the ohmic resistance and reactance of the barriers formed in the contact of the metal electrodes with the island film.

3. RESULTS OF MEASUREMENTS

The impedance spectra of the studied samples were measured at room temperature ~23°C and a relatively small amplitude of the ac voltage applied to the sample (0.7 V) in order to prevent the heating. It should be noted that the electric current flowing in the film structures under investigation always led the voltage in phase, which indicates a predominantly capacitive character of the reactive conductivity of the samples. As an example, Fig. 3 shows the frequency dependences of the impedance modulus $|Z|$ and the phase angle φ for the FeNi film with the thickness $h_2 = 1.6$ nm and the distance between electrodes $r = 10$ mm. It can be seen from this figure that, up to the frequency $f \sim 500$ kHz, the value of $|Z|$ corresponds to the ohmic

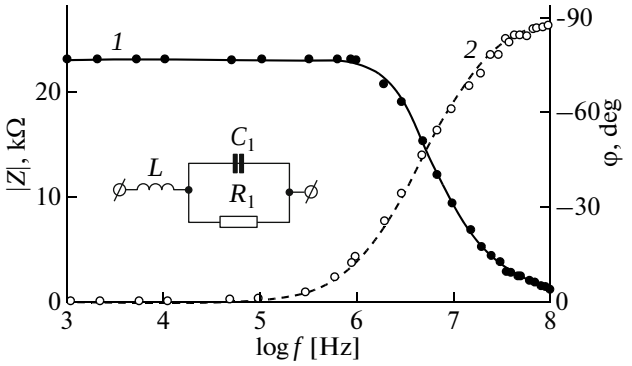

Fig. 3. Frequency dependences of (*1*) the impedance modulus $|Z|$ and (*2*) the phase angle φ of the 1.6-nm-thick FeNi film for the distance between electrodes $r = 10$ mm. The inset shows the model of the sample.

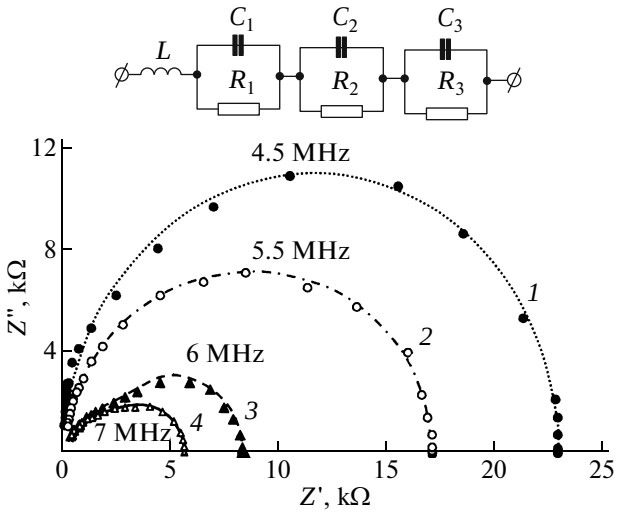

Fig. 4. Impedance loci of the 1.6-nm-thick film for different distances between electrodes $r =$ (*1*) 10, (*2*) 6, (*3*) 2, and (*4*) 1 mm. The frequencies corresponding to the positions of the maxima are indicated near the impedance loci. Points are experimental data, and lines represent numerical approximations according to the equivalent electrical circuit shown in the inset.

(active) resistance of the film, because the phase angle φ is close to zero. However, with a further increase in the frequency, the bias current begins to contribute to the admittance of the film and, at the highest frequencies where the phase angle reaches almost −90°, the impedance is completely determined by the reactive component of the conductivity (the electrical capacitance between islands of the film sample).

Figure 4 shows the impedance loci for the same sample, which were constructed for different distances (r) between the electrodes. It can be seen from this figure that impedance locus *1* represents a nearly regular semicircle with the center lying on the abscissa axis. This behavior of the impedance locus is characteristic of the electrical circuit shown in the inset to Fig. 3. The inductive element L connected in series with the parallel R_1C_1 circuit, in this case, simulates only the inductance of the lead wires. The calculation of the active and reactive elements in the circuit was performed according to the following expression for the complex impedance of the circuit:

$$Z^* = \frac{R_1(1 - j\omega R_1 C_1)}{1 + (\omega R_1 C_1)^2} + j\omega L, \qquad (1)$$

where ω is the circular frequency (rad/s).

It is obvious that the real and imaginary components of the impedance, in this case, should be expressed by the following relationships:

$$Z' = \frac{R_1}{1 + (\omega C_1 R_1)^2}, \qquad (2)$$

$$Z'' = \omega L - \frac{\omega C_1 R_1^2}{1 + (\omega C_1 R_1)^2}. \qquad (3)$$

The best agreement between the results obtained from measurements of the characteristics of the impedance and the calculation (see curves *1* and *2* in Fig. 3 and curve *1* in Fig. 4) is achieved with the following parameters of the equivalent electrical circuit shown in the inset to Fig. 3: $C_1 = 1.5$ pF, $R_1 = 22.9$ kΩ, and $L = 1.8$ μH. The relaxation time of this circuit is $\tau = RC = 3.44 \times 10^{-8}$ s. This value is close to the relaxation time calculated in accordance with the frequency corresponding to the observed maximum in the impedance locus $f_{max} = 4.5$ MHz (see Fig. 4, curve *1*): $\tau = 1/(2\pi f_{max}) = 3.54 \times 10^{-8}$ s.

As should be expected, with each decrease in the distance r between the electrodes of the sample under investigation, there occurs a monotonic decrease in the active resistance of the film. This resistance every time corresponds to the value at the point of intersection of each impedance locus in Fig. 4 with the abscissa axis on the right ($R_1 = Z'$ for $\omega \longrightarrow 0$). It is worth noting that, in this case, the frequencies corresponding to the maxima of the impedance loci are only slightly shifted toward the higher frequency range from 4.5 to 7.0 MHz. This suggests that, when the gap between the electrodes decreases, the decrease in the resistance of the sample region is almost completely compensated by the increase in the capacitance of the sample, thus providing a relatively small change in the relaxation time τ. It should be noted that this behavior of the relaxation time τ for the film with a thickness of 1.6 nm represents only a special case. For thinner and thicker samples, the relaxation times depend on the distance between the electrodes to a considerably greater extent. For example, in the film with a thick-

Table 1. Parameters of the elements of equivalent electrical circuits for different distances between electrodes r of the 1.6-nm-thick sample

r, mm	C_1, pF	C_2, pF	C_3, pF	R_1, kΩ	R_2, kΩ	R_3, kΩ
1	14.0	4.00	3.37	5.61	1.96	0.53
2	10.1	4.50	2.94	7.20	2.10	0.58
6	4.92	2.28	5.40	9.10	7.64	0.32
10	1.65	0	0	22.9	0	0

ness of 1 nm, when the distance between the electrodes r changes from 10 to 1 mm, the relaxation time τ decreases by a factor of approximately two (from 5×10^{-6} to 1×10^{-7} s). In the film with a thickness of 18 Å, the relaxation time τ changes more strongly (from 2.3×10^{-8} to 6×10^{-9} s).

It can be seen from Fig. 4 that, as the distance between the electrodes r decreases, the shape of the impedance locus becomes increasingly more asymmetric. In this respect, in order to determine the resistive–capacitive characteristics of the film region under investigation, the equivalent electrical circuit with the R_1C_1 elements, which is shown in the inset to Fig. 3, is supplemented by another one or two series-connected elements C_2R_2 and C_3R_3 (see inset to Fig. 4). The impedance in this case is calculated according to the formula

$$|Z| = \left| \frac{R_1}{1 + j\omega C_1 R_1} + \frac{R_2}{1 + j\omega C_2 R_2} + \frac{R_3}{1 + j\omega C_3 R_3} \right|. \quad (4)$$

The results obtained from the calculations of the impedance loci for different values of r are presented in Fig. 4 by different lines (curves *2–4*). The values of the corresponding active and reactive elements of the equivalent electrical circuits for the same values of r are listed in Table 1.

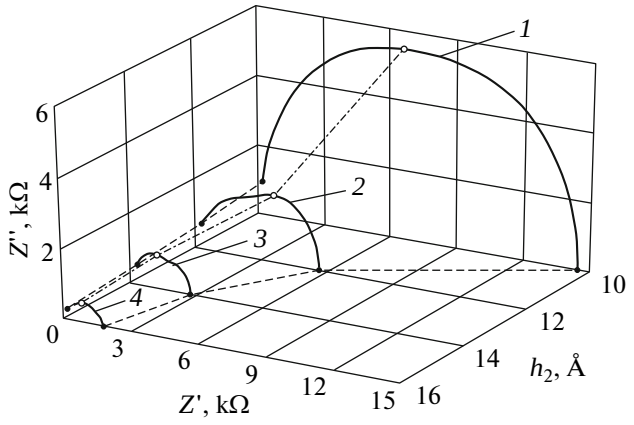

Fig. 5. Impedance loci for four thicknesses of the FeNi films: h_2 = (*1*) 1.0, (*2*) 1.2, (*3*) 1.4, and (*4*) 1.6 nm.

It can be seen that, with a decrease in the interelectrode gap from 10 to 1 mm, the capacitance C_1 of the first unit in the equivalent electrical circuit monotonically increases from 1.65 to 14.0 pF, whereas the corresponding resistance R_1, on the contrary, monotonically decreases from 22.9 to 5.61 kΩ. At the same time, there are no regularities revealed in the variations of the capacitances C_2 and C_3, as well as the resistances R_2 and R_3. This suggests that the R_1C_1 elements, most likely, simulate the "inner" part of the film sample between the contacts, whereas the R_2C_2 and R_3C_3 elements simulate the state of the contact areas. This assumption is also confirmed by the fact that the R_2C_2 and R_3C_3 elements are changed upon the replacement of gold-plated contacts by indium or graphite contacts; however, the specific feature observed in the behavior of the R_1C_1 elements remains completely unchanged. The analysis of the data presented in the table has demonstrated that the capacitance of the samples C_1 begins to exceed the capacitances of the contacts C_2 and C_3 only for gaps with $r \sim 1$–2 mm. These gaps can be considered to be optimum; hence, the subsequent measurements were performed using a gap with $r = 1$ mm.

Figure 5 shows the impedance loci obtained by the approximation of the measured impedance spectra with the use of the resistor–capacitor models of the studied FeNi films with different thicknesses $h_2 = 1.0$, 1.2, 1.4, and 1.6 mm. All samples have identical gaps between the measuring electrodes $r = 1$ mm. It can be seen from Fig. 5 that an increase in the thickness of the films leads to a decrease in both the active Z' and reactive Z'' components of their impedance, whereas the maxima of the impedance loci, which are indicated by open circles, monotonically shift toward the high-frequency range from 5 (for curve *1*) to 30 MHz (for curve *4*). For a number of measured samples with different thicknesses h_2, Table 2 presents parameters of the reactive C_1 and active R_1 elements of the equivalent electrical circuit of the interelectrode region with $r =$ 1 mm. The last column of this table contains the relaxation times. It can be seen that, with an increase in the thickness of the films from 1.0 to 1.8 nm, the capacitance C_1 monotonically increases from 5 to 20 pF,

which naturally can be associated with the increase in the number of islands and with the decrease in the distances between them. With a further increase in the thickness of the films, the process of coalescence of islands most likely begins to occur, which actually explains the slight decrease in the capacitance of the sample with a thickness of 2.0 nm.

Figure 6 shows the impedance loci for the studied film samples with the smallest thickness $h_2 = 0.7$ nm (Fig. 6a) and the largest thickness $h_2 = 5.0$ nm (Fig. 6b). The dashed line in Fig. 6a corresponds to the calculation of the impedance locus using the equivalent electrical circuit (see inset to Fig. 3) with the active resistance $R_1 = 120$ kΩ and the capacitance $C_1 = 4$ pF. In this case, the relaxation time of the sample can be easily estimated as $\tau = 4.8 \times 10^{-7}$ s. However, the experimentally measured part of the impedance locus for a "thick" sample shown in Fig. 6b could be approximated only using the equivalent electrical circuit with the frequency-dependent capacitance element (*CPE*) and the active resistance *R* (see inset to Fig. 6b). The impedance Z_{CPE} is determined by the following expression [17]:

$$Z_{CPE} = \frac{1}{Y_0(j\omega)^n}, \quad (5)$$

where Y_0 is the frequency-independent factor and n is the nonlinearity index of the capacitance element. By properly choosing the parameters of the equivalent electrical circuit for the best coincidence of its characteristics in the chosen part of the spectrum with the results of measurements (see Fig. 6b), we obtained the following values: $R = 578$ Ω, $Y_0 = 4$ pF, and $n = 0.85$. The presence of the nonlinear element *CPE* in the equivalent electrical circuit indicates that there is a set of relaxation times $\tau_i = R_iC_i$. The existence of this set of relaxation times can be associated with the large dispersion in the sizes of the islands due to their coalescence on some areas with the formation of significantly larger sized islands. The estimated average relaxation time of this sample is $\langle\tau\rangle \sim 2.5 \times 10^{-9}$ s.

4. DISCUSSION OF THE RESULTS

The permittivity of materials has been usually determined using the method based on the replacement of the air gap of a plane-parallel measuring capacitor by a sample under investigation. In this case, the permittivity is calculated as the ratio of the capacitance of the capacitor with the sample to the capacitance of the empty capacitor. However, in the case of our layered structure with a nanoisland metal film, this method is incorrect, because the distribution of the electric field in the substrate without a film and the distribution of the electric field in the layered film–substrate structure differ significantly. Therefore, in order to estimate the permittivity of the sample, it is necessary to use a method that makes it possible to calculate the capacitance of the layered substrate–FeNi-film structure with planar metal electrodes of the specified geometry. This calculation can be based on the conformal mapping method. The essence of this method is as follows. The electric field of a planar layered structure is transformed into an electric field generated by virtual plane-parallel capacitors which between their electrodes contain a substrate with the

Table 2. Dependence of the parameters of the equivalent electrical circuits on the film thickness h_2

h_2, nm	C_1, pF	R_1, kΩ	$\tau_{R_1C_1}$, 10^{-8} s
1.0	5	100	50
1.3	12	11	1.3
1.6	14	5.6	7.8
1.8	20	1.0	2
2.0	16	0.9	1.4

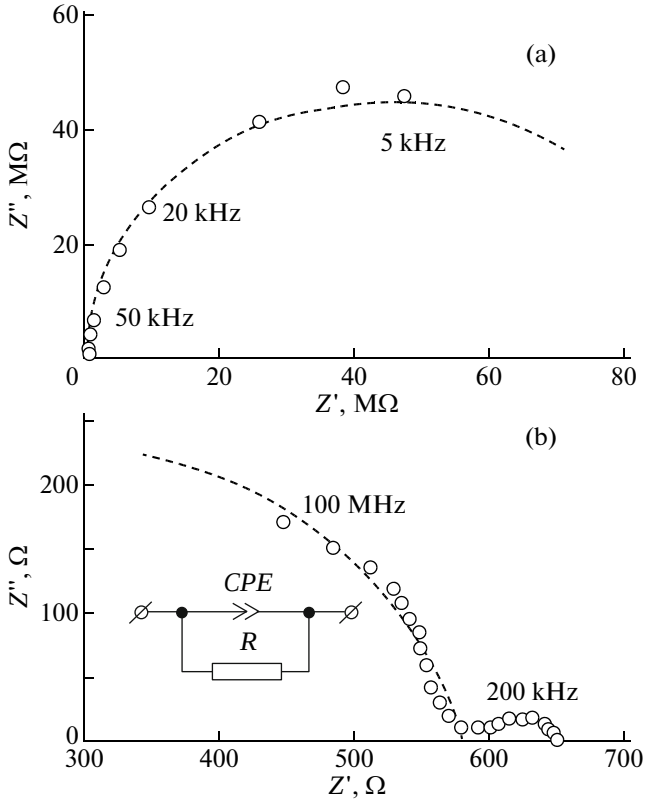

Fig. 6. Impedance loci of the FeNi films for (a) the thickness $h_2 \sim 0.7$ nm with the distance between electrodes $r = 1$ mm and (b) $h_2 = 5.0$ nm with $r = 10$ mm.

Table 3. Dependence of the permittivity on the thickness of the permalloy film

Parameter	Value			
h_2, nm	1.0	1.2	1.4	1.6
ε	2.0×10^7	9.5×10^7	1.1×10^8	1.2×10^8

permittivity ε_1, a film with the permittivity $\varepsilon_2 \gg \varepsilon_1$, and air with $\varepsilon = 1$ [18]. This method is referred to in the literature as the partial capacitance method.

Let us assume that, in the film sample with metal islands, the ac electric field is concentrated predominantly in the bulk of the film. Then, the capacitance C_1 of the layered structure (see Fig. 2) can be calculated according to the following simplified formula [19]:

$$C_1 = \varepsilon_0\left[\frac{\omega\varepsilon_1}{\pi}\ln\left(\frac{16(h_1-h_2)}{\pi r}\right) + \frac{(\varepsilon_2-\varepsilon_1)}{r/h_2 + (4/\pi)\ln 2}\right]. \quad (6)$$

Here, ε_0 is the dielectric constant of vacuum. This formula corresponds to a parallel connection of the capacitor of the substrate with the capacitor of the island structure. According to this relationship, we calculated the relative permittivity of the system of metal nanoislands forming a film with the average thickness of 1.6 nm and the distance between the electrodes $r = 1$ mm and obtained a very large value of the permittivity $\varepsilon_2 \approx 1.4 \times 10^8$. Since the frequency dependence of the impedance of the structures under investigation, as a rule, is adequately described by conventional electrical circuits based on lumped *RC* elements, it is obvious that the calculated values of the permittivity do not depend on the frequency.

It is interesting to note that the same high values of $\varepsilon \sim 10^7$–10^8 were obtained in [11] for single-layer and multilayer island structures based on Co, W, and FeNi. The permittivity in that work was calculated according to the following relationship:

$$\varepsilon_2 = \frac{C_1\varepsilon_1 h_1}{C_s h_2}, \quad (7)$$

where C_s is the capacitance between the measuring electrodes in the absence of the film, which, obviously, can be easily measured on a suitable sample specially prepared for such experiment. In our case, the structure without the film has a capacitance $C_s \sim 0.3$ pF for $r = 1$ mm. As a result, the permittivity calculated from formula (7) for the samples studied in our work also proved to be in the range $\varepsilon_2 \sim 10^7$–10^8.

Such high values of the dielectric constant are difficult to explain by a simple polarization of nanoislands, when the positive and negative charges appear on opposite sides of each individual island. In this case, the model of the sample can be represented in the form of a grid of capacitors connected in series and parallel. Then, the permittivity can be calculated for the actual sizes of these granular systems, which proves to be several orders of magnitude lower than that measured for real island films.

In order to explain the nature of the observed high permittivity of the studied thin permalloy films, we should also take into account other possible mechanisms of polarization in them, for example, those related to particular physical properties of metal islands on the substrate [20]. It is generally believed that the equilibrium state of the electron gas in small particles or islands without regard for thermal fluctuations is electroneutral. However, the existing dependence of the surface energy of the electron gas (at a level of the chemical potential) on the distance, shape, and size of the particles can lead to a redistribution of electrons between the islands. In this case, the minimum of free energy is reached when electrons of the particles with a high chemical potential μ transfer to particles with a lower chemical potential μ. As a result, the neighboring islands in a thin film are oppositely charged.

The redistribution of electrons between the islands can also be associated with other mechanisms; for example, the redistribution of electrons can occur through tunneling transitions. Actually, during tunneling transitions, charges can reside on an island for a relatively long time; consequently, the whole system of islands in the film also appears to be charged [11]. The occurrence of tunneling transitions of electrons through potential barriers between the islands proves that the electrical resistivity of the studied films exponentially decreases with increasing temperature.

Both in the first and the second of the aforementioned mechanisms, the neighboring pairs of positively and negatively charged islands can be considered as dipoles, which, due to the polarization, contribute significantly to the permittivity of the film.

It is obvious that the capacitance and permittivity of these structures should be determined by the concentration of charged islands, which increases with increasing thickness of the films. In confirmation of what has been said, Table 3 presents the relative permittivities ε for several studied films as functions of the film thickness h_2 for the distance between electrodes $r \sim 0.9$–1.2 mm, which were calculated from the measured values of the capacitance C_1 according to formula (6). It can be seen that, with an increase in the thickness of samples from 1.0 to 1.6 nm, the permittivity has a tendency toward an increase.

5. CONCLUSIONS

Thus, the frequency dependences of the impedance in the frequency range from 100 Hz to 100 MHz have been measured on samples of permalloy thin films with a nanoisland structure. It has been demonstrated that, for measurements of the impedance spectra of island structures in the aforementioned frequency range, the optimum thicknesses of the FeNi films lie in the range from 1.0 to 2.0 nm. The measurements of thinner films have been limited by instrumental capabilities because of the sharply increasing electrical resistance and the decrease in the capacitance between the islands. As regards the measurements of thicker samples, the time of their structural relaxation significantly decreases and the island structure gradually disappears.

In order to analyze the results of the measurements, we have considered models based on lumped element equivalent electrical circuits. The complex impedances of the films and times of their structural relaxation have been obtained. The methods used for determining the relative permittivity of the island films have been described. It has been found that the relative permittivity of the island films reaches very large values $\varepsilon \sim 10^7$–10^8. It has been shown that there is no dispersion of the permittivity of the island structures. Consequently, the samples under investigation are well simulated either by one equivalent *RC* circuit for thin samples, which is characterized by one relaxation time, or by several *RC* circuits for relatively "thick" samples characterized by a set of relaxation times.

The nature of the mechanisms, which provide a redistribution of electrons between islands of a permalloy thin film and thus endow the neighboring islands with charges of opposite signs, has been discussed. As a result, the "island film–dielectric substrate" structure can be considered as a grid of electric dipoles, whose polarization can explain such high values of the permittivity observed in the experiment.

ACKNOWLEDGMENTS

This study was supported by the Russian Federal Targeted Program "Scientific and Scientific–Pedagogical Human Resources for the Innovative Russia in 2009–2013," the Siberian Branch of the Russian Academy of Sciences (Integration research project no. 5), and the Presidium of the Russian Academy of Sciences (project no. 21.1).

REFERENCES

1. H. Gleiter, Acta Mater. **48**, 1 (2000).
2. R. A. Andrievskii, Ross. Khim. Zh. **XLVI** (5), 50 (2002).
3. B. A. Belyaev, A. V. Izotov, S. Ya. Kiparisov, and G. V. Skomorokhov, Phys. Solid State **50** (4), 676 (2008).
4. B. A. Belyaev, A. V. Izotov, and A. A. Leksikov, Phys. Solid State **52** (8), 1664 (2010).
5. N. Mott and E. Davis, *Electronic Processes in Non-Crystalline Materials* (Oxford University Press, Oxford, 1979; Mir, Moscow, 1982).
6. I. V. Zolotukhin, Yu. E. Kalinin, and A. V. Sitnikov, Priroda (Moscow) **91**, 24 (2001).
7. E. E. Starostin and A. G. Kolmakov, Fiz. Khim. Obrab. Mater., No. 5, 38 (1998).
8. P. N. D'yachenko and Yu. V. Miklyaev, Kompyut. Opt. **31**, 31 (2007).
9. P. A. Grünberg, *Nobel Lecture* (The Nobel Foundation, Stockholm, 2007).
10. H. Kubota, R. Sato, and T. Miyazaki, J. Magn. Magn. Mater. **167**, 12 (1997).
11. A. P. Boltaev and F. A. Pudonin, JETP **107** (3), 501 (2008).
12. R. V. Teleshin, *Thin Ferromagnetic Films* (Butterworth, London, 1964; Mir, Moscow, 1964).
13. E. Barsoukov and J. R. Macdonald, *Impedance Spectroscopy: Theory, Experiment and Application* (Willey, New York, 2005).
14. R. F. Soohoo, *Magnetic Thin Films* (Harper and Row, New York, 1965; Mir, Moscow, 1967).
15. G. V. Bondarenko and A. P. Dolgarev, in *Apparatus and Methods of X-Ray Analysis* (Mashinostroenie, Leningrad, 1983), p. 128 [in Russian].
16. A. K. Ivanov-Shits and I. V. Murin, *Solid State Ionics* (St. Petersburg State University, St. Petersburg, 2000), Vol. 1 [in Russian].
17. B. M. Grafov and E. U. Ukshe, *Electrochemical Circuits of the Alternating Current* (Nauka, Moscow, 1973) [in Russian].
18. O. G. Vendik, S. P. Zubko, and M. A. Nikol'skii, Tech. Phys. **44** (4), 349 (1999).
19. A. N. Deleniv, Tech. Phys. **44** (4), 356 (1999).
20. E. L. Nagaev, Sov. Phys.—Usp. **35** (9), 747 (1992).

Translated by O. Borovik-Romanova